SAND2022-14670C

Model Validation of a Modular Foam Encapsulated Electronics Assembly with Controlled Preloads Via Additively Manufactured Silicone Lattices

Tanner Ballance[1], Bryce Lindsey[2], Daniel Saraphis[3], Kevin Long[4], Moheimin Khan[4], Sharlotte Kramer[4], Christine Roberts[4]

[1]Purdue University
610 Purdue Mall
West Lafayette, IN, 47907

[2]Oklahoma State University
107 Whitehurst
Stillwater, OK, 74078

[3]The University of North Carolina at Charlotte
9201 University City Blvd
Charlotte, NC, 28223

[4]Sandia National Laboratories
P.O. Box 5800 – MS0840
Albuquerque, NM, 87185

ABSTRACT
Traditional electronics assemblies are typically packaged using physically or chemically blown potted foams to reduce the effects of shock and vibration. These potting materials have several drawbacks including manufacturing reliability, lack of internal preload control, and poor serviceability. A modular foam encapsulation approach combined with additively manufactured (AM) silicone lattice compression structures can address these issues for packaged electronics. These preloaded silicone lattice structures, known as foam replacement structures (FRS), are an integral part of the encapsulation approach and must be properly characterized to model the assembly stresses and dynamics. In this study, dynamic test data is used to validate finite element models of an electronics assembly with modular encapsulation and a direct ink write (DIW) AM silicone FRS. A variety of DIW compression architectures are characterized, and their nominal stress-strain behavior is represented with hyperfoam constitutive model parameterizations. Modeling is conducted with Sierra finite element software, specifically with a handoff from assembly preloading and uniaxial compression in Sierra/Solid Mechanics to linear modal and vibration analysis in Sierra/Structural Dynamics. This work demonstrates the application of this advanced modeling workflow and results show good agreement with test data for both static and dynamic quantities of interest, including preload, modal, and vibration response.

Keywords: Electronics Packaging, Additive Manufacturing, Foams, Model Validation, Vibration

INTRODUCTION

Electronic assemblies are among the most sensitive engineering hardware and their performance can be impacted heavily by damage induced by shock and vibration. Traditionally, techniques to protect electronic assemblies in harsh vibration environments typically involve the use of physically or chemically blown potted foams. While these techniques can be robust against vibration damage, some sacrifices are made for this protection. Firstly, once an electronic assembly is potted, servicing the assembly in the cases of short circuits, loose contacts or broken solders can be difficult or impossible as the assembly is completely encased by the potting material. Another downfall of this technique is manufacturing reliability. During the potting, many factors can play a role on how the assembly will

respond to vibrations including: curing temperature, chemical composition, and stresses generated by the curing or blowing of the potting material. Optimizing all these factors to achieve a desired response under vibrations poses a complex problem. If the blown foam generates too high of a pressure within the assembly, either through improperly chosen temperatures, densities, or chemistry, unwanted preload of the electronics can occur. With a lack of control on the preload of the electronics, mode shapes and resonances will be impossible to predict. To address these issues, a modular encapsulation approach is utilized in conjunction with additively manufactured (AM) silicone lattice compression structures, also known as foam replacement structures (FRS) [1]. The modular encapsulation approach reduces the effort to access electronics when in the assembly, drastically increases manufacturing repeatability and offers reasonable control on the preload conditions experienced by the electronics. It accomplishes this by taking advantage of AM techniques and design-oriented packaging.

Before these structures can be used in place of traditional techniques, the silicone lattice FRS must be properly characterized under preloaded conditions. Being a vital part of this alternative encapsulation technique, the FRS behavior will dictate the stresses and dynamics in the assembly. Essentially acting as a control input, the lattice structure and thickness of the silicone elastomeric material can affect not only the frequency of the dominant modes but also the magnitude of the response. Modifying the FRS thickness, lattice spacing, and angle can result in a different stiffness and as a result a different modal and vibration response

In this work, finite element (FE) models of an electronic assembly of microcontrollers (Raspberry Pis) with modular encapsulation and direct ink write (DIW) printed silicone structures are validated with static and dynamic test data. To ensure a reasonable computation time, the silicone lattice structures were homogenized as a bulk hyperfoam material. A variety of FRS are analyzed to ensure the hyperfoam model parameters properly capture the nominal stress-strain behavior of the DIW FRS. The modeling was conducted using the Sierra finite element software suite, where uniaxial compression was carried out in Sierra/Solid Mechanics (Sierra/SM) [2] and linear modal/vibration analysis was carried out in Sierra/Structural Dynamics (Sierra/SD) [3]. The structure of the paper is as follows: description of the hardware used in modeling and experiments, material parameterization, experimental methods, the specific simulations carried out along with results, and finally discussion and conclusions made about the validity of the finite element model.

GEOMETRY

The assembly of interest is composed of an aluminum enclosure consisting of a housing and lid, with electronics components encapsulated within the enclosure and by hyperelastic foams. The assembly is roughly 7 inches by 7 inches by 4 inches and is shown in Fig. 1.

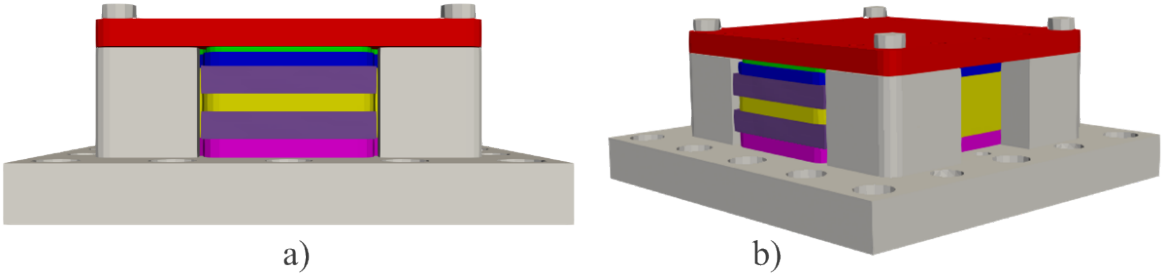

Fig. 1: Assembly side view (a) and isometric view (b)

Figure 2 shows a cross section of the assembly with the individual components labeled.

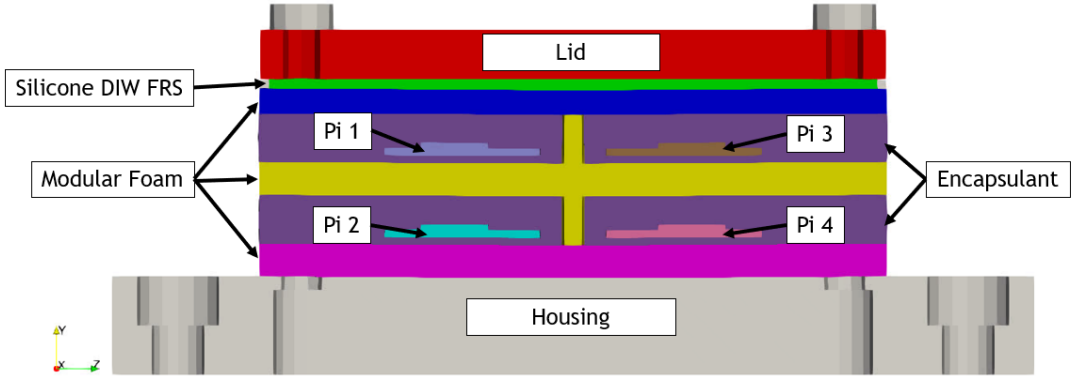

Fig. 2: Assembly cross section

The layout of the electronics within the assembly can be seen in Fig. 3. Stripping away the middle foam layers shows the four Raspberry Pi Zeros and cable connectors. The Pis are mounted at each corner using steel rods that extend from the housing plate. The Pis are protected by the modular foam layers and an elastomeric encapsulant. The assembly is closed using the DIW FRS under pressure to maintain layer contact.

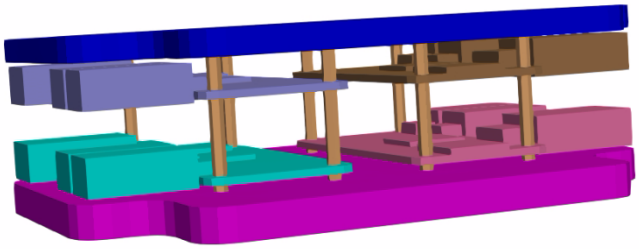

Fig. 3: Raspberry Pis (4) within the assembly

MATERIALS

Several materials are used within the assembly with very different mechanical properties. All materials are treated as homogenous continua including the DIW lattices (as direct numerical simulation of the lattice struts was prohibitively computationally expensive). Table 1 summarizes some of the nominal elastic properties of the materials used in the analyses.

Table 1: Material Elastic Properties

Name	Material	Young's Modulus (psi)	Poisson Ratio
Enclosure	Aluminum	10×10^6	0.33
Raspberry Pi	FR4	4.35×10^6	0.30
Modular Foam	PMDI	12.8×10^3	0.25
Encapsulation	Sylgard(R)184	366	0.4995

For both the Sierra/SM and Sierra/SD simulations, the aluminum enclosure material is modeled as linear elastic. The encapsulated Raspberry Pis and connectors are approximated as a single linear isotropic FR4 circuit board material and details of individual circuit elements, connectors, and solder connections are ignored.

The rigid internal foams are also treated as linear elastic with properties that correspond to a 11 pound per cubic foot rigid polymeric methylene diisocyanate (PMDI) foam. It is worth noting that the rigid foams studied here have yield strengths depending on density, so our analyses are only valid for stress states below yield of approximately 400 psi at room temperature [4]. The DIW lattice material is modeled with a hyperelastic, compressible Ogden model (hyperfoam), which is suitable for representing the rate independent mechanical behavior of compressible materials

[5]. Rate effects from viscoelasticity or pneumatic effects (air flow through the lattice) are not considered. We note that the lattice structures are always at most of cubic symmetry or lower, but we are focused on the uniaxial preloading response in this work and think an isotropic representation is reasonable. Details of the hyperfoam fit are provided in the following section. In the Sierra/SM simulation, the solid siloxane encapsulation was modeled with the Gent model [6] using a locking parameter of 3.65. This was simplified to a hyperelastic Neo-Hookean model for the structural dynamic simulations, which we think is suitable since the encapsulation is only expected to achieve moderate strains. The bulk and shear moduli for the Sylgard(R) 184 encapsulation were obtained from [7]. Finally, we note that the material properties and constitutive models are fully consistent between the structural mechanics and structural dynamics simulations for the hyperfoam models. A linearized material tangent stiffness based on the hyperfoam parameters from the material fit is utilized such that no new properties are defined when handing off the preloaded state to perform the modal and frequency response analyses.

HOMOGENIZED MATERIAL PARAMATERIZATION FOR DIW LATTICE STRUCTURES

A sufficiently accurate model for the 3D printed DIW silicone lattice structures that can represent preloads and the steady state vibration response of the assembly is required. Ideally, direct numerical simulation of the lattice would be included in the assembly model whereby the solid material would be represented either as a solid elastomer continuum or as a collection of beams. Either form of direct numerical simulation (DNS) was too expensive or full of additional challenges (beam on beam contact as well as short beam formulations). So, our approach was to homogenize the mechanical behavior of the DIW silicone lattice structures with the hyperfoam model mentioned in the previous section. That is, we fit the experimental uniaxial compression stress vs. strain (engineering) data at slow strain rates with the hyperfoam model. This exercise is trivial, but optimized parameter outputs often are unstable (lead to imaginary sound speeds as evidenced by negative eigenvalues of the acoustic tensor). So, we followed a procedure to fit each individual lattice separately and during the fitting process to check extensively if, under many different states of deformation, the material would have an acoustic tensor with negative or zero eigenvalues. Our procedure followed prior work detailed in [8].

A schematic of the DIW lattice structures with associated design parameters is shown in Fig. 4 which defines the printing parameters that control the lattice construction: the filament diameter, filament spacing, overlap, angle of each layer, and the number of layers in the thickness direction.

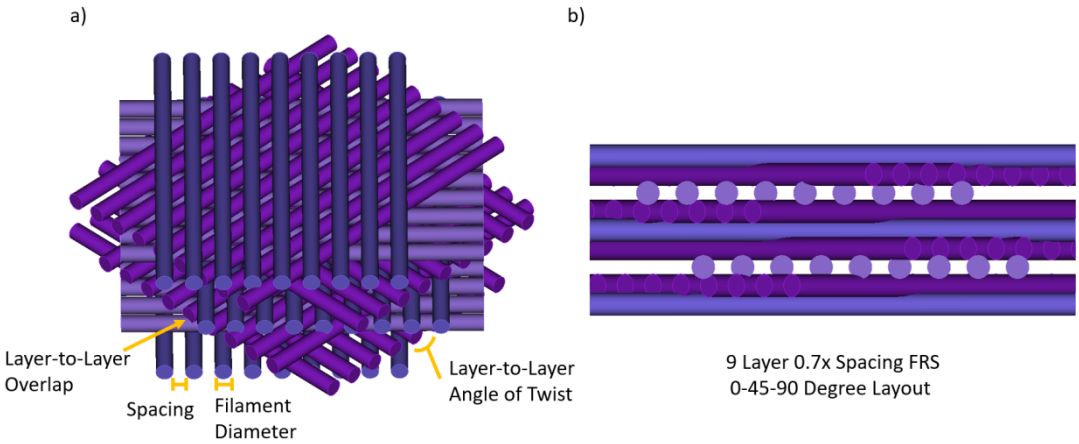

Fig. 4: Direct ink write silicone lattice structures (a) isometric view showing the printing parameters and (b) side view of 9 layer 0.7x overlap 0-45-90-degree FRS

Lattices analyzed here have a specific layup wherein each subsequent layer is rotated 45 degrees from the previous layer along the thickness direction. In all cases, 8-, 9-, and 11-layer structures were printed following the procedure outlined in [1]. Stiffer structures were of interest, so the filament spacing considered ranged from 0.7 to 0.9 times the filament diameter, and in certain cases, overlap between layers (which is nominally around 20%) was decreased to 12%. Despite different geometries, the different lattices showed two families of responses as shown in Fig. 5a with several repeats with highly stiff lattices realized for the 8 layer, 0.7 spacing and more compliant lattices realized for

the other printing parameters. Although close, it is worth noting that the lattice structures are not size converged. That is, for the same filament diameter and layer spacing, different numbers of layers produce slightly different nominal stress vs. strain relations. Consequently, each set of printing parameters must be fit with an individual model. All curves in Fig. 5a were fit following the procedure in [8], and a curve of relevance used in the experiments is shown in Fig. 5b.

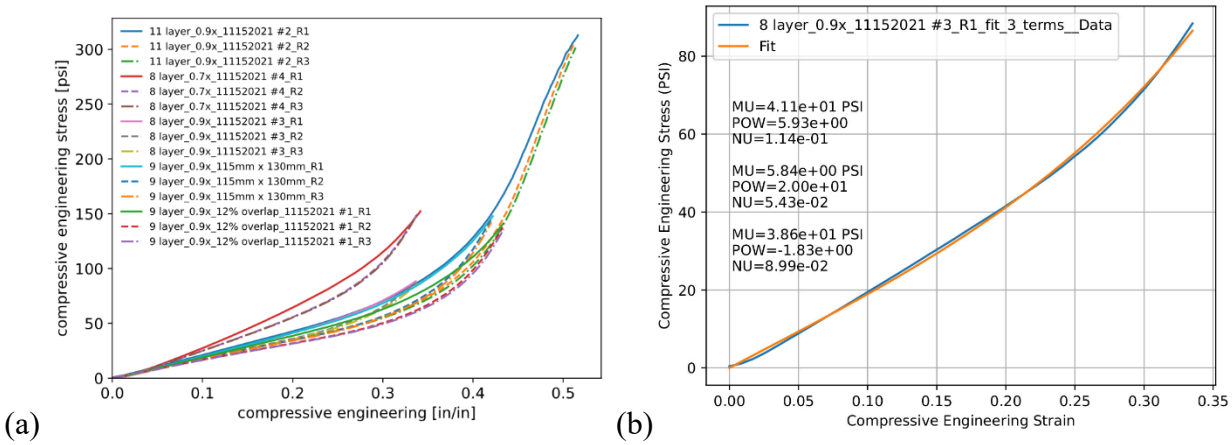

Fig. 5: 0-45-90 layups of 8, 9, and 11-layer lattice structures with different layer spacings, layer-to-layer overlaps, and repeats (a). A stabilized hyperfoam fit of the 8-layer, 0.9 spacing lattice used in subsequent sub-assembly preload and steady state vibration simulations.

EXPERIMENTAL METHODS

Several units in various assembly configurations were tested, two of which are discussed here. These two nominally identical units were tested to assess unit-to-unit variability. Both quasistatic and dynamic testing was done to experimentally characterize the assemblies. First, the units were assembled and preloaded using a uniaxial testing machine. Load-displacement behavior of each assembly was recorded for various thicknesses of the DIW silicone lattice FRS as shown in Fig 6. The 0.0875-inch thick FRS are the focus of this work.

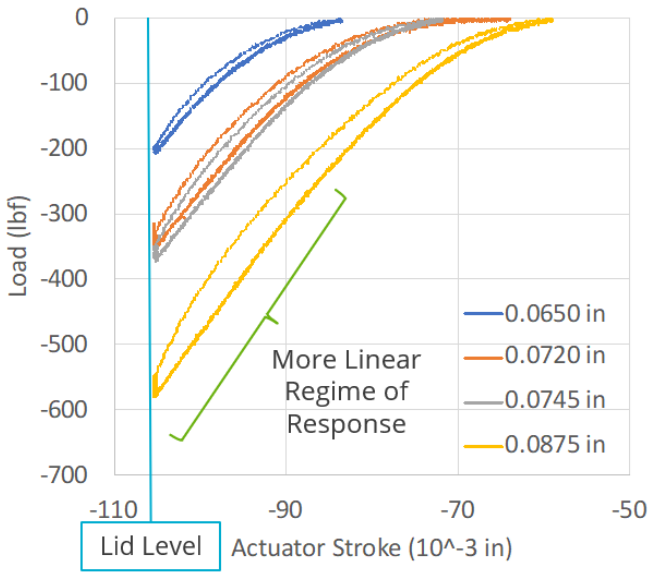

Fig. 6: Test load-displacement curves for various FRS thicknesses

Following the compression to lid level, the bolts for each of the units were torqued down to retain the lid preload. After the assembly preload, free-free modal testing was conducted. Triaxial accelerometers were placed on the external

metal housing as well as a single uniaxial accelerometer on each of the four Raspberry Pis, as shown in Fig. 7. The first 3 experimentally measured free-free mode frequencies and damping ratios are summarized in Table 2. The second mode (bottom plate drumming) is emphasized as it is the primary mode of interest for this work.

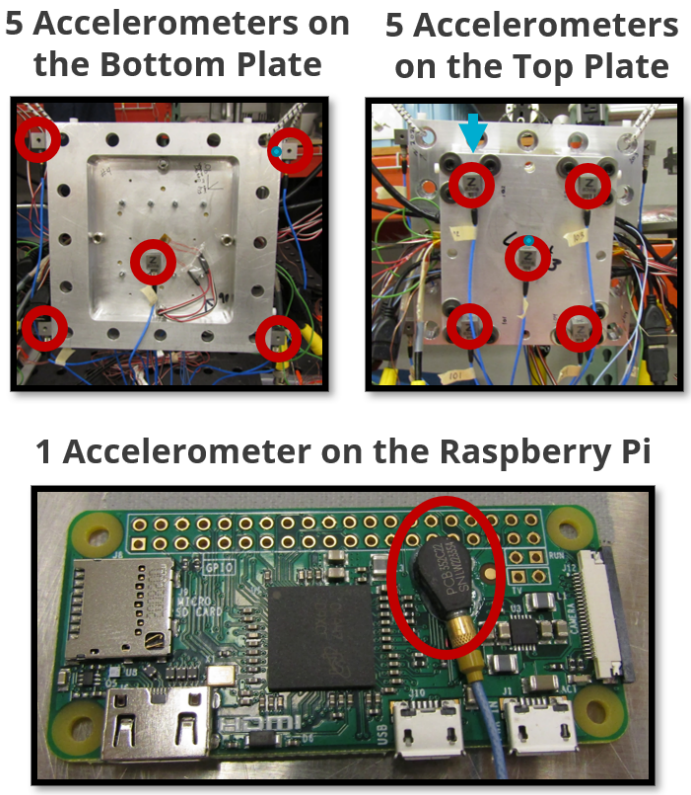

Fig. 7: Modal test setup and accelerometer placement

Table 2: Free-Free Modal Results for Tested Units

Mode	Description	Unit 1 Freq. (Hz)	Unit 1 Damp. (%)	Unit 2 Freq. (Hz)	Unit 2 Damp. (%)
1	Board Out-Of-Phase Bouncing	1233	9.97	1458	6.54
2	**Bottom Plate Drumming**	**1390**	**4.84**	**1526**	**5.84**
3	Assembly Torsion	1720	1.02	1716	0.85

Uniaxial vibration testing was also conducted on each assembly using an electrodynamic shaker. An image of the test setup is shown in Fig. 8. A low-level random vibration was applied to the base of the assembly, corresponding to the Y-direction in Fig. 2. The in-axis acceleration response of the Raspberry Pis was measured using the same uniaxial sensor as in the modal test.

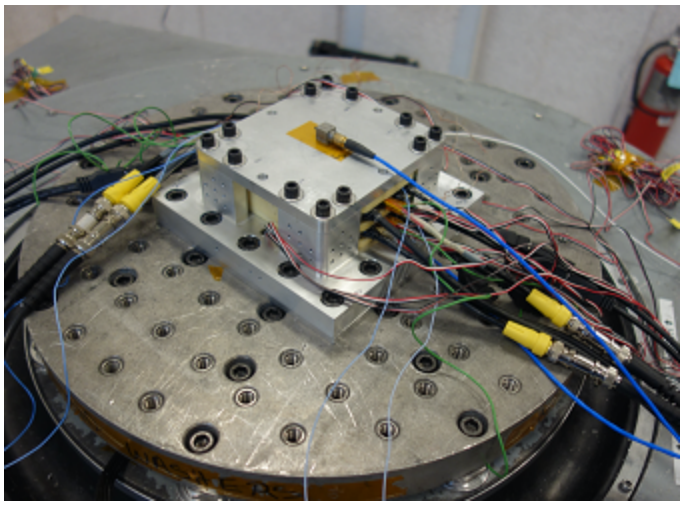

Fig. 8: Vibration Testing Setup

FINITE ELEMENT ANALYSIS

A finite element model of the assembly was developed to match the as-tested configurations and the experimental data was used to validate the model. Both static and dynamic simulations were performed based on the experimental procedures discussed in the prior section. A nonlinear Sierra/SM finite element model was used to perform the preloading, and linear modal and random vibration analyses were subsequently performed with Sierra/SD. Figure 9 demonstrates this analysis workflow.

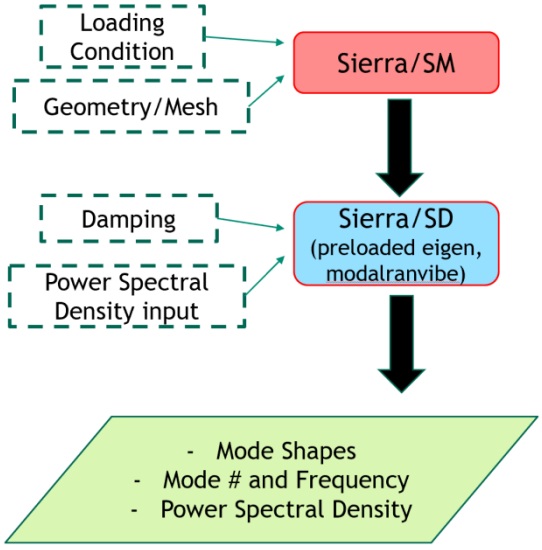

Fig. 9: FEA Workflow

In the SM finite element model, the bottom surface of the assembly was fixed in the direction of loading, and a cosine ramp function was used to prescribe the lid displacement required to close the gap created by the homogenized FRS. Then, an artificial strain was applied to the bolt shanks to close the gap. The SM model is considered quasi-static in that the preload is applied over a long enough time such that the kinetic energy is small with respect to internal energy. The finite element model uses an explicit time marching algorithm to resolve the preload on the FRS. A selective deviatoric solid element formulation was adopted for the eight-node hexahedral (Hex8) elements defined as solid sections. The strain incrementation was defined to be strongly objective. The model contains approximately 73,000 Hex8 elements for a total of 105,000 nodes. A reference image of the assembly showing the scale of the element size can is provided in Fig. 10. CUBIT meshing software was used to mesh the assembly [9].

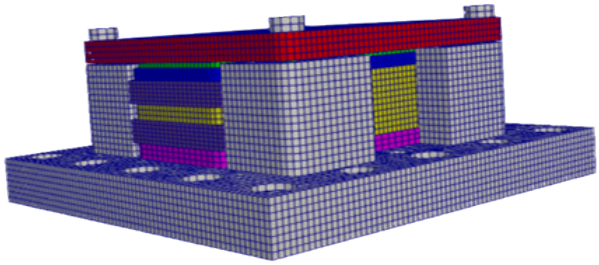

Fig. 10: Meshed assembly showing element size relative to total size.

The resulting state of the preloaded SM simulation is handed off and linearized to perform SD simulations. Namely, the material tangent stiffnesses are updated and the eigenfrequencies, eigenmodes, and system accelerations due to a random input are determined. The boundary condition used in the SD simulation is an applied acceleration to the bottom surface of the enclosure which coincides with the direction of the height of the assembly. The acceleration is applied to the bottom surface via a point mass attached to the surface by a rigid bar. The acceleration is specified by assigning a specific mass and magnitude to the point mass. The applied acceleration is modulated between 0 Hz and 2000 Hz with a spectral density amplitude of 0.01 g^2/Hz. The applied acceleration matches the excitation used for experimentation on the assemblies. Fixed base eigenfrequencies and mode shapes are computed up to 3000 Hz to reduce the effects of modal truncation in the random vibration solution.

The main interest of this work is to validate the model workflow and investigate the effects of preloading the assembly with the DIW FRS on the dynamic response of the electronics. To this end, the main results of interest in the SM simulation were checks to see if the loading and boundary conditions were satisfactory when compared to data from the quasistatic experiments. Namely, that the forces used to compress the assembly were consistent with those from experiments. The key information gathered in the SM simulations were comparing force and lid displacement, as well as checks on the contact enforcement, such as contact force and status. As for the subsequent SD analyses, the free-free modes can be compared to the test data for each unit, along with comparisons of acceleration response of the Raspberry Pis due to fixed base random vibration input.

RESULTS

As discussed previously, the focus of the SM analysis was to ensure proper preload of the assembly. This preload was quantified by computing the internal reaction force of the lid as it closed the gap. This can be compared to the experimentally measured load displacement behavior, specifically the final preload force. Figure 11 shows the lid force vs time and force displacement behavior during preloading. Results were filtered to 4 kHz using a 4th order Butterworth filter.

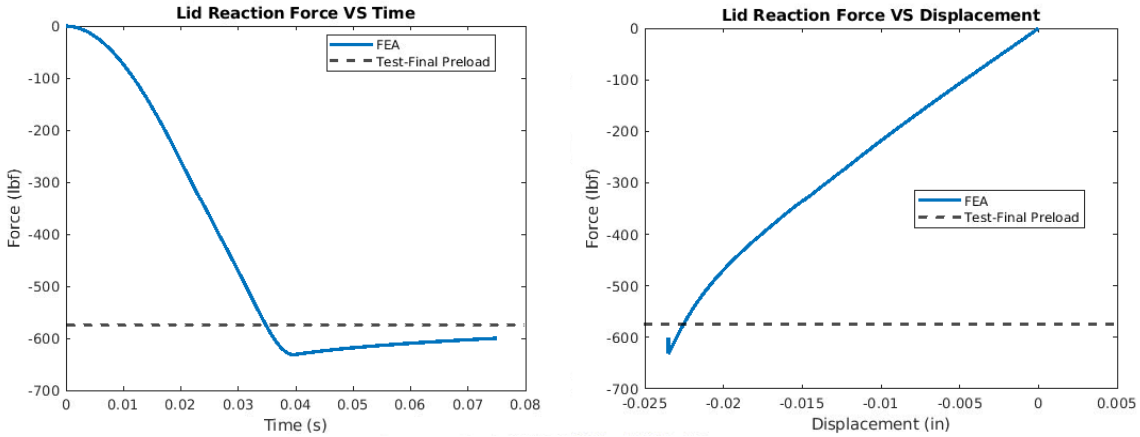

Fig. 11: Lid force vs time and Lid reaction force vs displacement

At the end of the preloading portion, the lid reaction force reaches close to 650 lb_f and eventually falls back to around 600 lb_f after the settling step of the simulation. Note that longer relaxation of the materials was not considered due to computational limitations, however this would affect the final preload value. Still, the preload value from the SM simulations is close to the experimentally measured value of 575 lb_f for the 0.0875-inch FRS, as given in Fig. 6 in the experimental methods section. In addition, the shape of the force-displacement curve resembles test data. Along with the lid force displacement information, contact checks were performed to ensure proper gap closure and the resulting preloaded state from the SM simulation was determined to be satisfactory.

Next, the final step from the Sierra/SM simulation was handed off to Sierra/SD, which linearized the preloaded state for computing the modal analysis. Fig. 12 shows the preloaded fixed base and free-free housing plate drumming modes of the assembly. The free-free value of 1443 Hz is comparable to the experimental results for the test units 1 and 2-1390 Hz and 1526 Hz, respectively.

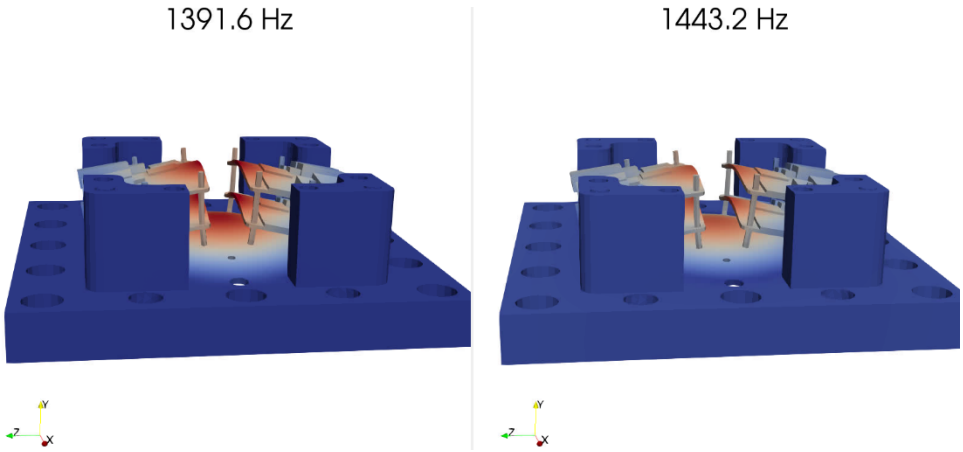

Fig. 12: Preloaded fixed base (a) and free-free (b) housing drumming mode

The fixed base FE modal solution was then used to perform the random vibration analysis using the test loading discussed previously. A value of 2% uniform damping was used in the analysis, with added damping based on the modal test values, for example 5% damping applied specifically to the drumming mode of interest. Figure 13 shows the comparisons between the FE model and the test data for each unit. Results are presented for two Raspberry Pis, one at the top (Pi 2) and one at the bottom (Pi 3) of the assembly, matching the layout shown in Fig 2.

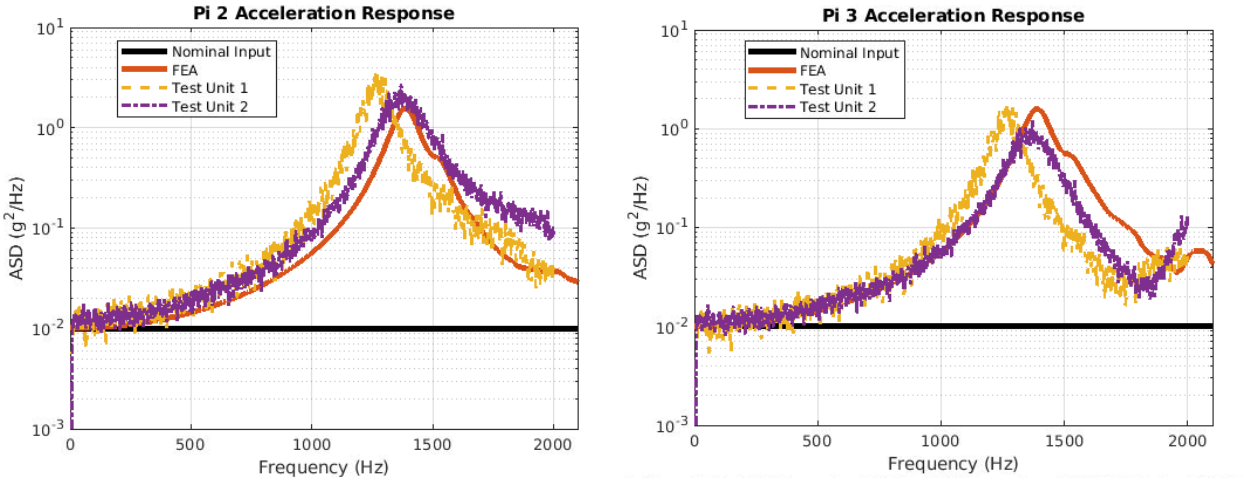

Fig. 13: Pi 2 and Pi 3 acceleration response comparison

The acceleration response of the FE model for both Pi 2 and Pi 3 is consistent with the experimental data for both units. The plots highlight the dominant in-axis response of the drumming mode discussed previously and the simulation captures that behavior well. Table 3 summarizes the free and fixed frequencies for this mode, using the modal data along with peak response frequency as an estimate.

Table 3: Drumming mode frequency comparison

Unit	Free-Free Frequency (Hz)	Fixed-Base Frequency (Hz)
FE Model	1443	1392
Test Unit 1	1390	~1265
Test Unit 2	1526	~1370

Although the simulation results do not track either of the tested units exactly, the initial and peak responses are in-family, especially given the observed unit to unit variability in the drumming mode frequency and damping. There are some discrepancies at higher frequencies for Pi 3, but it is difficult to make further comparisons since the vibration data stops at 2 kHz.

It is important to note that the geometry and material simplifications could have contributed to the model being slightly stiff. However, both the static and dynamic analysis results tracked well with the experimental data, providing good validation for the presented modeling workflow for modular foam assemblies with DIW silicone lattices.

CONCLUSION

This work presents model validation for an analysis workflow involving an electronics assembly with a modular encapsulation and additively manufactured silicone lattice foam replacement structures. Using homogenized representations of the AM FRS, hyperfoam parameterizations were obtained and a nonlinear Sierra/SM model was developed, which showed comparable load-displacement behavior to test data during preloading. The preloaded state was handed off to a linearized Sierra/SD model, which accounted for updated material stiffnesses and showed modal and vibration results that matched well with experimental data.

The modular approach for electronic assemblies discussed in this work demonstrates advantages over the traditional techniques due to the ability to control on the dynamic response of the electronics. Future work will explore various thicknesses and designs of the lattice structures and investigate the effect of varying levels of preload on the static and dynamic response of the assembly. Furthermore, additional correlation and test activities could help address the observed discrepancies and improve the model representation.

ACKNOWLEDGMENTS

The authors would like to thank Janelle Lee and Brian Owens for their work on initial design, modeling, and simulation, Steven Carter for the modal testing, and Matthew Campisi for the vibration testing of the assembly.

REFERENCES

[1] Roach, D. J., et al., Utilizing computer vision and artificial intelligence algorithms to predict and design the mechanical compression response of direct ink write 3D printed foam replacement structures, Additive Manufacturing, Volume 41, 2021, 101950, ISSN 2214-8604, https://doi.org/10.1016/j.addma.2021.101950.

[2] Sierra Solid Mechanics Team. 2022. "Sierra/SolidMechanics 5.10 User's Guide.". United States. https://doi.org/10.2172/1886996. https://www.osti.gov/servlets/purl/1886996.

[3] Sierra Structural Dynamics Team. "Sierra/SD - User's Manual - 5.10.". United States. https://doi.org/10.2172/1887938. https://www.osti.gov/servlets/purl/1887938.

[4] Lame Team, Library of Advanced Materials for Engineering 5.6, SAND2022-3247, 2022

[5] Storakers, B. On material representation and constitutive branching in finite compressible elasticity, Journal of Mechanics and Physics of Solids, Volume 34, Issue 2, 1986, 125-145

[6] Gent, A. N., A new constitutive relation for rubber. Rubber Chemistry and Technology, 69(1), 59-61.

[7] Long, K. N. and Brown, J. A., A Linear Viscoelastic Model Calibration for Sylgard 184, SAND2017-4555

[8] Long, K. N. and Hamel, C. M., Stabilized Hyperfoam Modeling of the General Plastics EF4003 (3 PCF) Flexible Foam. SAND2022-7395R

[9] CUBIT Development Team, CUBIT Geometry and Mesh Generation Toolkit 15.8 User Documentation, 2021, SAND2021-5152 W.